Effects of Antenna Polarization on Power and RMS Delay Spread in LOS/OOS Indoor Radio Channel

Z. Y. Liu, L. X. Guo, W. Tao, and C. L. Li
School of Science, Xidian University
Box 274, No.2, Taibai Road
Xi'an 710071, China

***Abstract*-The ray tracing (RT) method offers significant advantages in terms of the accurate and comprehensive prediction of radio channel characterization in indoor environments. As a consequence, this paper presents results of computer simulation based on a three-dimensional (3D) RT method for various directional polarized antennas, where the effects of antenna polarization on power and RMS delay spread are investigated in line-of-sight (LOS) and out-of-sight (OOS) indoor channel. These results indicate that the difference in predicted power between cross-polar case and copular case, under LOS environment, is more noticeable than that of OOS case. Whereas，the difference in predicted RMS delay spread between cross-polar and copular case, under OOS environment, is more noticeable than that of LOS case.**

I. INTRODUCTION

The forthcoming years, the market for indoor wireless networking facilities is expected to grow considerably in both commercial and domestic sectors [1]. Thus, a thorough investigation of indoor propagation channel characteristics represents a fundamental step toward the design and the implementation of such applications [2]. This makes it necessary to have an accurate propagation to predict propagation channel characteristics in indoor environment. Deterministic methods as ray tracing (RT) are a good alternative to be used [3]. RT is a commonly used computational method for site-specific prediction of the radio channel characteristics of wireless communication systems. The RT technique inherently provides time delay and angle of arrival information for multipath reception conditions [4].

Due to the advantage of the RT model, researchers have sought to use this model as a crucial reference to investigate the indoor and outdoor propagation channel characteristics. In [5], the influence of building shape near the corner and its electrical properties on the ray-tracing predictions are presented. The shape is shown to have an important role in accurately predicting both received power and delay spread. Rizk et al. [6] study the influence of database accuracy on two-dimensional (2D) RT-based predictions in urban microcells. The work reported in [7] presents results of computer simulation based on a three-dimensional (3D) RT method for various directional polarized antennas, where the effects of polarization, antenna directivity, and room size on delay spread are investigated in the line-of-sight (LOS) indoor channel.

The current study, based on the RT model that have been proven and proposed in [8], is focused on investigating effects of antenna polarization on power and RMS delay spread in LOS/ out-of-sight (OOS) indoor cases. This paper is organized as follows. The used indoor RT model is introduced in Section II. The main focus is described in Section III, where power and RMS delay spread for both transmitter (Tx) and receiver (Rx) with two polarizations (vertical and horizontal linear) is predicted. Finally, the conclusions are drawn in Section IV.

II. INDOOR RAY TRACING MODEL

The RT model used in the present study considers the following ray paths:

1) direct rays as line-of-sight,
2) ray paths with all possible combinations of reflected rays on vertical facets, transmitted rays on vertical indoor objects and diffracted rays on vertical edges,
3) ray paths containing all ray paths belonging to type 1) with one additional reflection on the floor,
4) ray paths involving all ray paths belonging to type 2) with one additional reflection on the ceiling,
5) all possible combinations of reflected rays on both floor and ceiling and transmitted rays on indoor objects with one additional wall reflection or not,
6) single-reflected ray paths on horizontal facets (roofs) belonging to indoor objects,
7) single-diffracted ray paths on horizontal edges.

In order to improve the efficiency of finding propagation paths, all propagation paths mentioned above are divided into four major categories (i.e., ray category I, II, III, and IV). And, different methods are used to deal with different ray categories. Based on creating virtual source tree [9] in which the relationship between neighbor nodes is left-son-and-right-brother one, all the propagation paths belonging to ray category I can be found out. All the propagation paths included in ray category II can be easily and rapidly determined by using the geometry principle presented in [10] and doing necessary intersection tests. Due to only taking into account one order reflection or diffraction, the computational cost determining both ray category III and IV can be ignored. Other details about the the 3D RT model can be obtained in [8].

Once all ray paths from Tx to Rx are determined, the

contribution of each path can be expressed as

$$E = \frac{E_0 f_t f_r \cdot e^{-jkr}}{r} \cdot \prod_{i=1}^{n} R_i \cdot \prod_{s=1}^{u} T_s \cdot \prod_{l=1}^{m} \left(D_l A_l^d \right), \quad (1)$$

where

k	propagation constant;
E_0	reference field;
f_t and f_r	transmitting and receiving antenna field radiation patterns in the direction of the ray, respectively;
r	path length;
A_l^d	spreading factor for lth diffraction;
n, m, and u	total number of reflections, diffractions, and transmissions, respectively;
R_i, D_l, and T_s	reflection coefficient for the ith reflector, diffraction coefficient for the lth diffracting wedge, and transmission coefficient for the sth transmission, respectively (the calculation of the three coefficients can be traced in [11], [12]).

According to the results calculated in Eq. (1), the contribution of each propagation path to the received power can be calculated using the following expression [13]:

$$P_r = P_t G_t G_r \left(\frac{\lambda}{4\pi} \right)^2 \left| \frac{E_r}{E_i} \right|^2, \quad (2)$$

where

E_i	$\sqrt{(\eta_0/4\pi) P_t G_t}$;
η_0	$\sqrt{\eta/\varepsilon} \approx 120\pi$ = intrinsic impedance;
$P_{t,r}$	transmitted and received power, respectively;
$G_{t,r}$	transmitter and received gain, respectively;
E_r	total electric field at receiver.

All rays contributing significantly to the channel characterization at the examined position must be traced, and the complex impulse response of the radio channel is then found as the sum of these contributions [14]

$$h(t) = \sum_{i=1}^{N} A_i \delta(t - \tau_i) \exp(-j\vartheta_i). \quad (3)$$

Here, the received signal $h(t)$ is formed by N time delayed impulses (rays), each represented by an attenuated and phase-shifted version of the original transmitted impulse. The amplitude A_i, arrival time τ_i and phase ϑ_i of each ray are calculated by Eq. (1) and path length r.

III. Simulation and Discuss

In order to analyze the effects of antenna polarization on RMS delay spread in LOS/OOS indoor radio channel based on the 3D RT model introduced in Section II, a practical complex indoor environment is investigated in this section. The geometrical model of this indoor environment is shown in Fig. 1, including the floor and ceiling in order to consider the reflections produced in both. The room dimensions are width 7.9 m, length 17.9 m, and height 3.85 m. For this study, not only are the windows and doors included in the environment database, but also the tables and all major metallic objects. This indoor environment is also used to demonstrate the accuracy of the proposed 3D RT method, and details about the geometrical features can be obtained in [15].

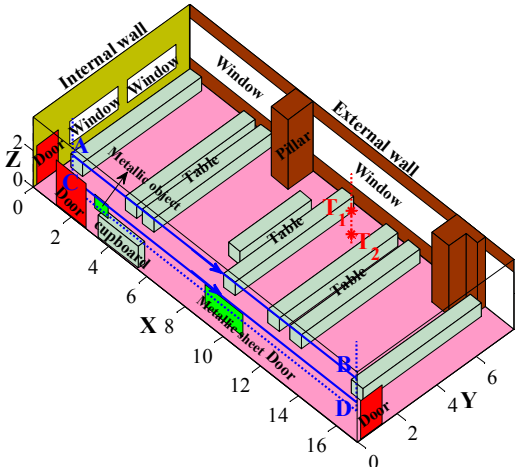

Fig. 1. 3D representation of the office.

In our calculation, two antenna positions are considered and are individually mounted at 1.8 m (located at T_1) and 0.5 m (located at T_2) above the floor. The carrier frequency of the two antennas are 2.4GHz and transmitted power are 20 dBm. Two sets of Rxs are distributed with constant spatial steps (chose as 0.2 m in the paper) along route AB (1.8 m high) and route CD (0.5 m high), respectively. For each route (15.0 m long) 76 prediction points are calculated. Both the transmitting and receiving antennas are typical half wavelength polarized dipoles. The two transmitting antennas are vertical polarization, while receiving antennas have both vertical polarization (parallel to the z-axe) and horizontal polarization (parallel to the x-axe). The material characteristics used in this study are shown in Table I. All the electrical properties and characteristics of the indoor environment elements, such as doors, windows, tables, cupboards and so on, are set by referring [1], [16].

TABLE I
The Material Characteristics Used in This Study

	Relative permittivity	Conductivity (S/m)
concrete (pillars, external wall, and the ceiling)	9	0.1
Plasterboard (internal walls)	2.8	0.1
Floor covered with marble	7	0.00022
Glass (windows)	6.67	10^{-10}
Wood (doors)	3.72	4.6×10^{-4}
Metallic sheet	3	100
Metallic object	1	3.23×10^{5}
Chipboard (tables and cupboard)	2	0.015

A. *Simulations for LOS Case*

Fig. 2 shows the predicted power along the route AB in LOS indoor environment. It can be seen that the power curve for copular case have the same trend as that of cross-polar case. However, the average of predicted power for copular case is about 30 dBm more than that of cross-polar case.

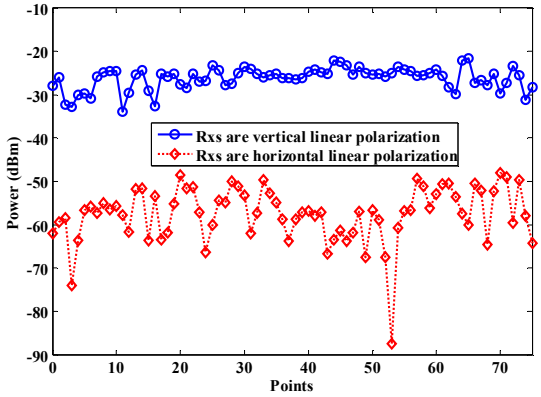

Fig. 2. Power for receivers along the route AB with two polarizations in LOS case, and Tx is located at T_1.

Fig. 3 illustrates the effects of antenna polarization on RMS delay spread in LOS indoor radio channel. Comparisons with results about predicted power shown in Fig. 2，the curves of delay spread for the two polarizations show better agreement, except for the middle of the route AB. This phenomenon occurs because the stronger signal with short delay is given up for cross-polar case.

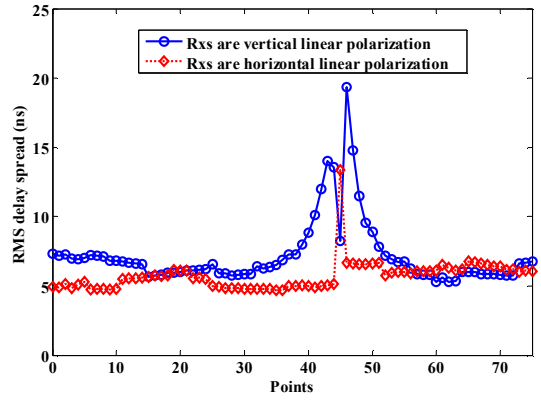

Fig. 3. RMS delay spread for receivers along the route AB with two polarizations in LOS case, and Tx is located at T_1.

B. *Simulations for OOS Case*

As indicated in Fig. 4, the difference in predicted power between cross-polar and copular case is not noticeable in contrast to the simulation results shown in Fig. 2. So, we can presume that directions of the electromagnetic field for propagation paths are rotated through undergoing multiple reflections on the facet, diffractions on the edges, or the combinations of them.

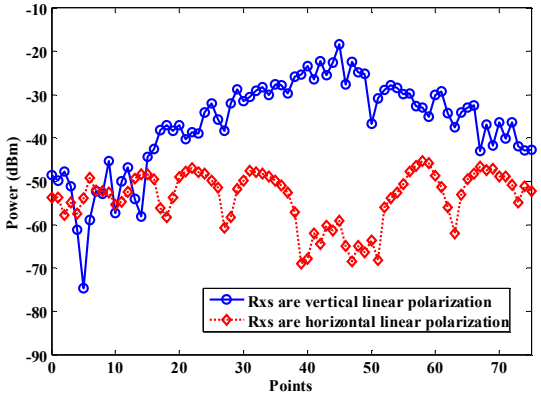

Fig. 4. Power for receivers along the route CD with two polarizations in OOS case, and Tx is located at T_2.

RMS delay spread for receivers along the route CD with two polarizations in OOS case is present. The trends of power curves for the two polarizations are opposition with each other. This proves that the directions of the electromagnetic field for propagation paths are rotated in OOS indoor environment. As for both LOS and OOS cases, the environment elements (tables, cupboard, and so on) more or less rotate the directions of the electromagnetic field, change the phase of each propagation path, and weaken the power taken by the path.

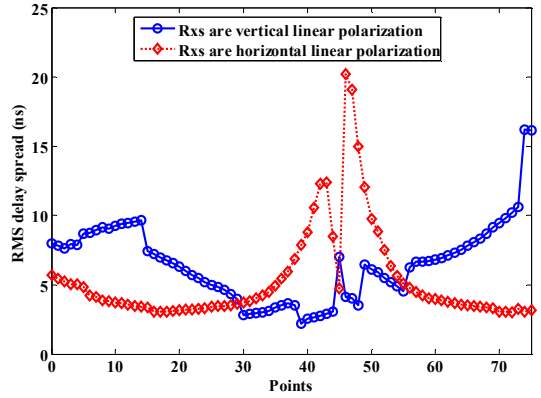

Fig. 5. RMS delay spread for receivers along the route CD with two polarizations in OOS case, and Tx is located at T_2.

IV. CONCLUSIONS

In this paper, a new 3D indoor ray-tracing model, which can be applied to any complex indoor propagation environment, is presented. Based on a technique where multiple reflections, transmissions and diffractions are considered via the ray-path classification into four different categories, the used model implements different methods to deal with different ray categories. Utilizing this model, the effects of antenna polarization on power and RMS delay spread in LOS/OOS indoor radio channel are investigated. Simulation results indicate that for OOS cases, directions of the electromagnetic field for propagation paths are evidently rotated to varying degrees. Therefore, the signal arriving at Rx is not always the strongest for the copular case, especially in OOS indoor

environment. Furthermore, the difference in predicted power between cross-polar and copular case, under LOS environment, is more noticeable than that of OOS case. Whereas，the difference in predicted RMS delay spread between cross-polar and copular case, under OOS environment, is more noticeable than that of LOS case.

ACKNOWLEDGMENT

This work was supported in part by the Fundamental Research Funds for the Central Universities (Grant No. K50513100013), the National Science Foundation for Distinguished Young Scholars of China (Grant No. 61225002) and the Foundation of Huawei Technologies CO., Ltd. (Contract No. YBWL2010247).

REFERENCES

[1] G. E. Athanasiadou and A. R. Nix, "A novel 3-D indoor ray-tracing propagation model: The path generator and evaluation of narrow-band and wide-band predictions," *IEEE Trans. Veh. Technol.*, vol. 49, no. 4, pp. 1152-1168, July 2000.

[2] V. Degli-Eposti, G. Lombardi, C. Passerini, and G. Riva, "Wide-band measurement and ray-tracing simulation of the 1900-MHz indoor propagation channel: Comparison criteria and results," *IEEE Trans. Antennas Propag.*, vol. 49, no. 7, pp. 1101-1110, July 2001.

[3] J. H. Jo, M. A. Ingram and N. Jayant, "Deterministic angle clustering in rectangular buildings based on ray-tracing," *IEEE Trans. Commun.*, vol. 53, no. 6, pp. 1047 - 1052, June 2005.

[4] K. A. Remley, H. R. Anderson and A. Weisshar, "Improving the accuracy of ray-tracing techniques for indoor propagation modeling," *IEEE Trans. Veh. Technol.*, vol. 49, no. 6, pp. 2350-2357, Nov. 2000.

[5] H. M. El-Sallabi, G. Liang, H. L. Bertoni, I. T. Rekanos, and P. Vainikainen, "Influence of diffraction coefficient and corner shape on ray prediction of power and delay spread in urban microcells," *IEEE Trans. Antennas Propag.*, vol. 50, no. 5, pp. 703-712, May 2002.

[6] K. Rizk, J. F. Wagen and F. Gardiol, "Influence of database accuracy on two-dimensional ray-tracing-based predictions in urban microcells," *IEEE Trans. Veh. Technol.*, vol. 49, no. 2, pp. 631-642, 2000.

[7] A. Kajiwara, "Effects of polarization, antenna directivity, and room size on delay spread in LOS indoor radio channel," *IEEE Trans. Veh. Technol.*, vol. 46, no. 1, pp. 169-175, Feb. 1997.

[8] Z. Y. Liu, L. X. Guo, X. Meng, and Z. M. Zhong, "A novel 3D ray-tracing model for propagation prediction in indoor environments," in *10th International Symposium on Antennas, Propagation & EM Theory*, Xi'an, China, 2012, pp. 428-431.

[9] Z. Y. Liu and L. X. Guo, "A quasi three-dimensional ray tracing method based on the virtual source tree in urban microcellular environments," *Prog. in Electromagn. Res.*, vol. 118, pp. 397-414, 2011.

[10] Z. Ji, B. Li, H. Wang, H. Chen, and T. K. Sarkar, "Efficient ray-tracing methmods for propagation prediction for indoor wireless communications," *IEEE Antennas Propag. Mag.*, vol. 43, no. 2, pp. 41 - 49, Apr. 2001.

[11] H. M. El-Sallabi and P. Vainikainen, "Improvements to diffraction coefficient for non-perfectly conducting wedges," *IEEE Trans. Antennas Propag.*, vol. 53, no. 9, pp. 3105-3109, Sept. 2005.

[12] S. Y. Seidel and T. S. Rappaport, "Site-specific propagation prediction for wireless in-building personal communication system design," *IEEE Trans. Veh. Technol.*, vol. 43, no. 4, pp. 879-891, Nov. 1994.

[13] S. Y. Tan and H. S. Tan, "A microcellular communications propagation model based on the uniform theory of diffraction and multiple image theory," *IEEE Trans. Antennas Propag.*, vol. 44, no. 10, pp. 1317-1326, Oct. 1996.

[14] G. L. Turin, F. D. Clapp, T. L. Johnston, S. B. Fine, and D. Lavry, "A statistical model of urban multipath propagation," *IEEE Trans. Veh. Technol.*, vol. VT-21, no. 1, pp. 1-9, Feb. 1972.

[15] Z. Y. Liu, L. X. Guo and X. Meng, "A novel 3D ray-tracing model for indoor propagation coverage prediction," *Journal of the Optical Society of America A*, (submitted).

[16] M. C. Lawton and J. P. McGeehan, "The application of a deterministic ray launching algorithm for the prediction of radio channel characteristics in small-cell environments," *IEEE Trans. Veh. Technol.*, vol. 43, no. 4, pp. 955-969, Nov. 1994.